On the Origin of the Optical Properties of Humic Substances

ARTICLE *in* ENVIRONMENTAL SCIENCE AND TECHNOLOGY · AUGUST 2004

Impact Factor: 5.33 · DOI: 10.1021/es049912h · Source: PubMed

2 AUTHORS, INCLUDING:

Rossana Del Vecchio
University of Maryland, College Park
23 PUBLICATIONS **1,271** CITATIONS

SEE PROFILE

Environ. Sci. Technol. **2004**, *38,* 3885−3891

On the Origin of the Optical Properties of Humic Substances

ROSSANA DEL VECCHIO† AND NEIL V. BLOUGH*

Department of Chemistry and Biochemistry, University of Maryland, College Park, Maryland 20742

Absorption and fluorescence spectroscopy and laser photobleaching experiments were employed to probe the origins of the optical properties of humic substances (HS). Luminescence quantum yields and the wavelengths of maximum emission were acquired for Suwannee River humic acid (SRHA) and fulvic acid (SRFA) at an extensive series of excitation wavelengths across the ultraviolet and visible. Laser irradiation at a series wavelength across the ultraviolet and visible was further employed to destroy selectively chromophores absorbing at specific wavelengths, using absorption spectroscopy to follow the absorption losses with irradiation time. The results provide unequivocal evidence that the absorption and emission spectra of these materials cannot result solely from a simple linear superposition of the spectra of numerous independent chromophores. Instead, the long wavelength absorption tail of HS (>350 nm) appears to arise from a continuum of coupled states. We propose that this behavior results from intramolecular charge−transfer interactions between hydroxy−aromatic donors and quinoid acceptors formed by the partial oxidation of lignin precursors. We further propose that these donor−acceptor interactions may be a common phenomenon, occurring within all natural hydroxy− or polyhydroxy−aromatic polymers that form appropriate acceptors upon partial oxidation. Examples of such species include lignin, polyphenols, tannins, and melanins.

Introduction

Humic substances are complex organic materials found ubiquitously in nature where they play an essential role in numerous environmentally important processes (*1*−*4*). Because light absorption by these substances increases exponentially with decreasing wavelength across the visible (VIS) and ultraviolet (UV) spectrum (*5*−*9*), they can provide aquatic organisms protection from damaging ultraviolet radiation (*7*, *9*−*11*). At the higher levels often found in fresh and coastal waters, absorption by HS can also dominate total light absorption in the blue portion of the visible spectrum, thus altering the quantity and quality of light available for photosynthesis (*4*, *7*, *12*, *13*). Through their effect on the aquatic light field, as well as through their photochemical reactions (*14*−*16*), HS can have a substantial impact on the biogeochemistry of natural waters (*7*, *14*).

Exhibiting no distinct bands, the absorption spectra of HS decrease with increasing wavelength in an approximately exponential fashion, whereas the emission spectra, which are broad and featureless, decrease in intensity and shift continuously to the red with increasing excitation wavelength (*17*). Although these properties of HS have been known and studied extensively for over 50 years (*1*, *2*, *4*, *7*, *17*−*19*), an adequate explanation of these spectral dependencies has yet to be achieved. In particular, no satisfactory explanation has yet been provided that can account for the long wavelength absorption and emission properties of these materials. Moreover, little is known at the molecular level about the nature of the constituents or interactions that produce these rather unique spectral features.

Recently, workers have begun to test whether the optical properties of HS can be attributed to a simple sum of the spectra of a series of independent chromophores or whether a more complex situation is occurring (*20*−*27*). The observed optical properties of HS could arise in two distinct fashions. The first postulates that the absorption (and emission) spectrum results from a simple linear superposition of the absorption (emission) spectra of an ensemble of independent (noninteracting or electronically isolated) chromophores (superposition model) (*20*, *22*, *23*). In contrast, the second postulates the presence of only a few distinct chromophores or closely related classes of chromophores, which through electronic interaction produce new optical transitions that are responsible for the exponentially decreasing, long wavelength absorption tail (interaction model) (*17*, *20*, *21*, *25*, *28*). Optical charge−transfer bands, produced via a ground-state interaction between an electron donor, D (e.g., polyhydroxylated aromatics, phenols, or indoles), and an electron acceptor, A (e.g., quinones), in close proximity represent a possible explanation for this long wavelength absorption (*17*, *21*, *25*, *27*−*32*). These donor−acceptor complexes are known to exhibit new broad absorption bands (at lower energies) that are not shown by either donor or acceptor molecules independently (*29*, *33*).

In earlier work (*21*), we provided preliminary evidence that the absorption spectra of HS cannot arise from a superposition of the spectra of numerous independent chromophores, based on an analysis of the photobleaching kinetics of HS and natural waters from the Delaware and Chesapeake Bays. Further, an attempt to account for the photobleaching behavior of these samples under polychromatic light using a superposition model was unsuccessful (*20*). Here, we employ room-temperature absorption and fluorescence spectroscopy and laser photobleaching experiments to test this idea explicitly. Luminescence quantum yields and the wavelengths of maximum emission for Suwannee River fulvic acid (SRFA) and humic acid (SRHA) were acquired at excitation wavelengths across the ultraviolet and visible wavelengths. A laser was further employed to destroy selectively species absorbing at specific wavelengths across the ultraviolet and the visible, using absorption spectroscopy to follow the photobleaching. Because HS could sensitize the photobleaching through the production of reactive oxygen species (*5*, *16*, *17*, *21*, *34*−*37*), samples were prepared in a high viscosity glycerol/water solution to minimize this possibility. This study provides unequivocal evidence that the absorption and emission spectra of these materials cannot arise solely from a simple superposition of the spectra of numerous independent chromophores. Instead, the long wavelength absorption tail of HS (>350 nm) appears to arise from a continuum of coupled states, which we attribute to intramolecular charge−transfer interactions within these materials.

* Corresponding author e-mail: nb41@umail.umd.edu; phone: (301)405-0051; fax: (301)314-9121.

† Present address: Earth System Science Interdisciplinary Center (ESSIC), 2207 Computer and Space Science Building, University of Maryland, College Park, MD.

10.1021/es049912h CCC: $27.50
Published on Web 06/09/2004

TABLE 1. Experimental Conditions for Luminescence Measurements

sample	concn (mg/L)	λ_{exc}
SRFA	2.5	280−320
	5.0	330−375
	25.0	380−445
	100.0	450−495
	200.0	500−600
SRHA	3.33	280−360
	10.00	365−495
	66.70	500−600

Experimental Procedures

Reagents. Glycerol (spectrophotometric grade) was obtained from Aldrich. Water was obtained from a Milli-Q Plus purification system (Millipore). Suwannee River fulvic acid (SRFA) and Suwannee River humic acid (SRHA) were obtained from the International Humic Substances Society. Quinine sulfate was obtained from MC/B.

Apparatus. A Hewlett-Packard 8452A and Shimadzu 2401-PC spectrophotometers were employed to acquire UV−visible absorption spectra. Absorption spectra were recorded against water over the range 200−800 nm.

An Aminco-Bowman AB-2 luminescence spectrometer (monochromator excitation and emission band-passes set to 4 nm) was employed for the fluorescence measurements. The excitation wavelength (λ_{exc}) was incremented every 10 nm over the range 280−350 nm and every 5 nm over the range 355−600 nm, with the emission spectra then recorded from 10 nm greater than λ_{exc} to 700 nm (see Table 1). The spectra were corrected for the instrument response using factors supplied by the manufacturer.

A Continuum Surelite II-10 Nd:YAG laser was employed as the source in the photobleaching experiments. To obtain additional irradiation wavelengths, the Nd:YAG laser was employed to pump a tunable ND6000 dye laser (see Supporting Information for details). The laser wavelengths spanned the UV to the visible wavelength (266−318−355−390−460−532 nm). The laser repetition rate was 10 Hz, and its output was reported in mJ/pulse.

Procedure: (A) Optical Measurements. SRFA and SRHA were dissolved in Milli-Q water to the appropriate concentrations (2.5−200 mg/L and 3.3−66.7 mg/L, respectively), and the absorption of each solution was recorded. Lower concentrations of SRFA and SRHA were employed to acquire emission spectra at shorter excitation wavelengths (Table 1) thereby eliminating inner filter effects. The SRFA (and SRHA) concentrations were successively increased to acquire fluorescence emission spectra at longer excitation wavelengths (Table 1), thus allowing for a more accurate determination of the absorbance at the excitation wavelength (for the quantum yield measurement) and for the emission spectra to be acquired at enhanced signal-to-noise ratios. Spectra were acquired with a 1 cm optical cell using Milli-Q water as blank. The blank was recorded in the same fashion as the samples and subtracted from each sample. Luminescence quantum yields (Φ) were obtained as reported previously (*8*, *38*).

(B) Laser-Photobleaching Measurements. SRFA and SRHA were dissolved in 90% glycerol/10% Milli-Q water to appropriate concentrations (10 or 50 mg/L) for the laser photobleaching experiments. The absorption spectra of SRFA and SRHA obtained in the glycerol/water solution were unaltered from those acquired in water. The higher concentration of SRFA and SRHA (50 mg/L) was employed during experiments at longer irradiation wavelengths (λ_{irr} >355 nm), thus providing higher absorbance at the longer wavelengths. The glycerol/water solution was employed as the blank, treated in the same way as the samples, and subtracted from the samples for each measurement.

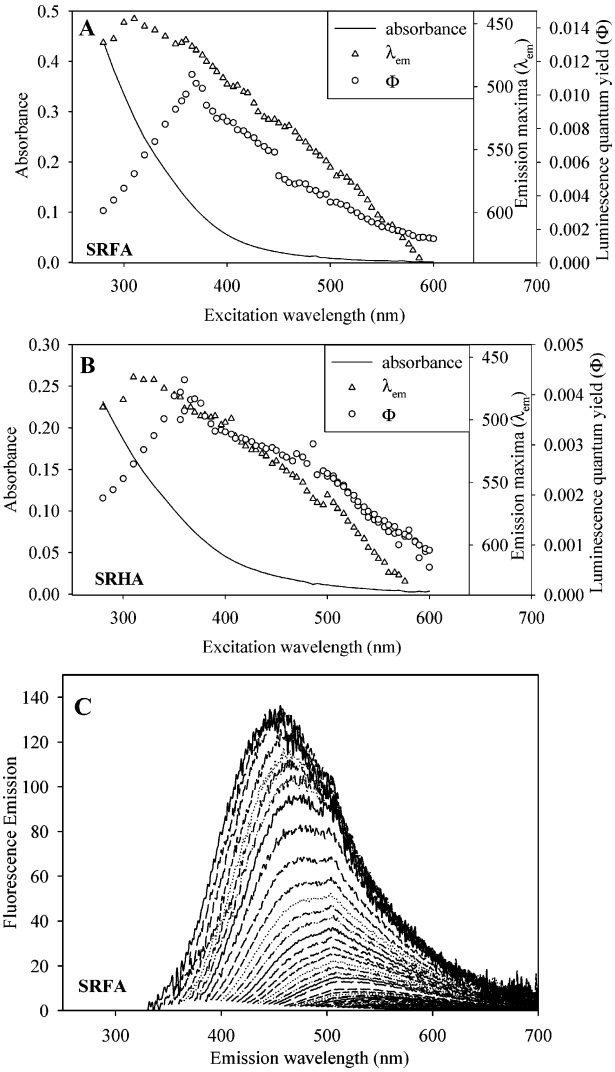

FIGURE 1. SRFA and SRHA optical properties. (A) (SRFA) and (B) (SRHA): absorption (−−); emission maxima, λ_{em} (λ_{exc} 280−600 nm) (Δ); and luminescence quantum yield (Φ) (○). (C) Corrected fluorescence emission spectra of SRFA (λ_{exc} 320−600 nm). SRFA and SRHA concentrations: (i) 25 and 10 mg/L, respectively, for absorption spectra; (ii) concentrations reported in Table 1 for fluorescence emission and quantum yields.

Laser photobleaching experiments were conducted at 266, 318, 355, 390, 460, and 532 nm. About 1.5 mL of solution (samples and blank) were placed in a 1 cm spectrophotometric cell and exposed to the laser source, with absorption spectra of the samples and blank collected as a function of irradiation time. The experiments were conducted until the sample absorbance decreased to <50% of its original value at λ_{irr}.

The absorbance lost during irradiation, ΔA, was calculated by subtracting the absorbance at time t, $A(t)$, from the original at time zero $A(0)$, while the absorbance at time t, $A(t)$, was divided by the original absorbance, $A(0)$, to provide F′, the fraction of original absorbance.

Results

Optical Measurements. As with most HS, the absorption spectra of SRFA and SRHA decreased in an approximately exponential fashion with increasing wavelength and exhibited no distinct absorption bands (Figure 1A,B). As reported previously (*17*, *39*), the absorption by SRHA, which has a

higher average molecular weight than the SRFA, extends to longer wavelengths at equivalent mass concentrations of SRFA and SRHA. At excitation wavelengths (λ_{exc}) between 290 and ~350 nm, the emission maxima (λ_{em}) remained approximately constant at ~450 nm for SRFA and ~460 nm for SRHA but then shifted continuously to the red with increasing λ_{exc} (Figure 1A,B). In contrast, the luminescence quantum yields (ϕ) increased from λ_{exc}= 290 nm to a maximum at λ_{exc} ~350 nm (ϕ_{SRFA} ~0.01 and ϕ_{SRHA} ~0.004), then decreased monotonically with increasing λ_{exc} (Figure 1A,B).

With few exceptions, luminescence originates from the lowest energy excited state (e.g., either the singlet or triplet); both λ_{em} and ϕ are therefore independent of excitation wavelength for an individual chromophore. Thus, both the continuous shift to the red of λ_{em} and the monotonic decrease of ϕ at λ_{exc} >350 nm indicates that individual chromophores cannot be resolved or isolated spectrally within our 5 nm resolution, implying further that there is a (near-) continuum of emitting species or states. Importantly, the emission envelope observed for spectra acquired at longer λ_{exc} always fell within the emission envelope of spectra acquired at shorter λ_{exc} (Figure 1C). This result suggests that the emitting species populated by longer wavelength excitation are a lower energy subset of those populated by shorter wavelength excitation. Consistent with the laser photobleaching results provided next, these data suggest that the long wavelength absorption and emission spectra of HS (>350 nm) originate from a coupled manifold of states.

A superposition model in which numerous discrete chromophores absorb and emit light independently of one another cannot readily accommodate these results. First, the continuous shift of the emission maximum to the red and the concomitant decrease in quantum yield implies the presence of a continuum of emitting species. Second, within a superposition model, the monotonically decreasing values of ϕ with increasing λ_{exc} would require uniquely that chromophores absorbing at successively longer wavelengths have lower ϕ. As pointed out previously for the photobleaching of HS (*21*), there is no fundamental reason to expect that discrete organic compounds absorbing at successively longer wavelengths would have systematically lower luminescence quantum yields. Indeed, most aromatic or heteroaromatic organic compounds that do absorb in the visible have relatively large fluorescence yields (*30*, *31*). In contrast, the magnitude of ϕ is extremely low in the visible (Figure 1A,B), which is unlike most organic chromophores ($\pi \rightarrow \pi^*$ transition).

Laser Photobleaching Measurements. Absorption Loss (ΔA). The loss of absorption produced by laser irradiation of SRFA and SRHA at selected wavelengths across the visible and ultraviolet (532, 460, 390, 355, 318, and 266 nm) was followed spectrophotometrically. To ensure that the observed absorption losses did not result in part from reactions with intermediates produced by the primary photochemistry (i.e., sensitized photobleaching), the HS were dissolved in a solution of 90% glycerol/10% water. There are excellent reasons to expect that the sensitized destruction of chromophores via diffusing reactive (oxygen) intermediates will be substantially suppressed in this medium. First, reaction of all diffusing intermediates will be slowed substantially due to the high viscosity. Second, highly oxidizing species such as the hydroxyl and alkoxyl radicals, as well as less reactive species such as peroxyl radicals, are likely to react exclusively with the glycerol due to its high concentration, producing far less reactive species such as superoxide and peroxides, which are much less likely to initiate chromophore bleaching. Control experiments using model compounds provide supporting evidence that sensitized photobleaching is not an important process in this medium (see Supporting Information).

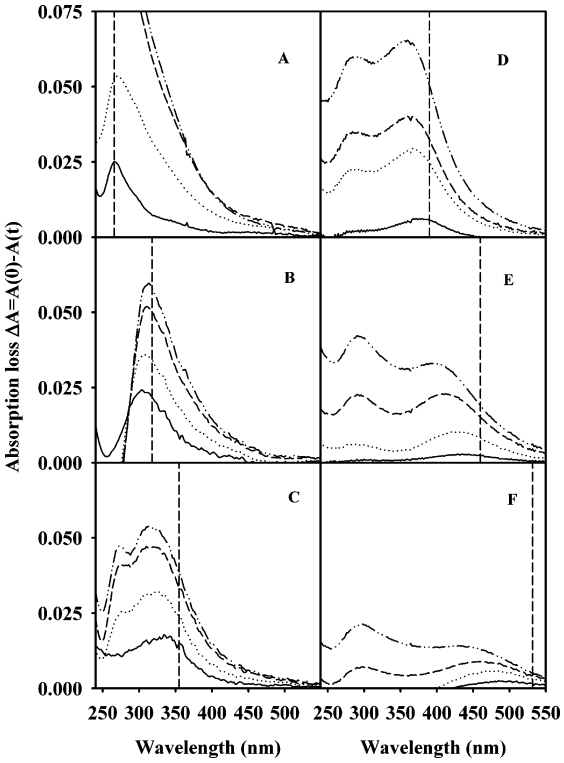

FIGURE 2. Time dependence of the absorption loss (ΔA) for SRFA upon exposure to laser irradiation (10 Hz): (A) at 266 nm (35 mJ/pulse) (10−580 s); (B) at 318 nm (6 mJ/pulse) (5−252 min); (C) at 355 nm (68 mJ/pulse) (2−85 min); (D) at 390 nm (5 mJ/pulse) (3−215 min); (E) (460 nm) (10 mJ/pulse) (0.3−312 min); and (F) (532 nm) (220 mJ/pulse) (10−3420 s). Vertical dashed lines represent irradiation wavelengths. Irradiation times: t_1 (—), t_2 (·····), t_3 (−−), t_4 (−··−).

The spectral loss of absorption for these HS varied both with the laser irradiation wavelength (λ_{irr}) and time (t) (Figures 2 and 3). At $\lambda_{irr} \geq$390 nm, absorption was first lost in a band centered at or very near λ_{irr} (Figures 2D−F and 3D−F; t_1, solid line). At longer times, this band broadened and shifted to the blue, while a second band of absorption loss appeared at ca. 300 nm (Figures 2D−F and 3D−F; t_2−t_4, broken lines). Unlike the bands formed near λ_{irr}, which blue-shifted with irradiation time, the 300 nm band exhibited a constant peak maximum.

Irradiation at 355 nm provided results similar to those obtained for $\lambda_{irr} \geq$390 nm, except that the 300 nm band was not clearly resolved due to its proximity to the irradiation wavelength. Irradiation first induced loss at the λ_{irr}, which at later times extended to longer wavelengths without the formation of any distinct bands (Figures 2C and 3C). Irradiation into the 300 nm band (318 nm) also produced a loss at long wavelengths without the formation of distinct bands, but now clear evidence for the production of new species absorbing at λ <300 nm (~250−260 nm) was obtained as shown by the negative ΔA for SRFA (Figure 2B) and the lower losses of absorption at longer irradiation times for SRHA (Figure 3B). Similarly, irradiation at 266 nm produced an absorption loss at long wavelengths without the appearance of distinct bands, as well as evidence of the production of species absorbing at short wavelengths, <250 nm (Figures 2A and 3A).

The 300 nm band was produced at all $\lambda_{irr} \geq$390 nm, indicating that all species absorbing within this spectral region are coupled electronically with the 300 nm band. Consistent with this view, irradiation into the 300 nm band (λ_{irr} = 318 nm) produced a substantial or complete loss of absorption

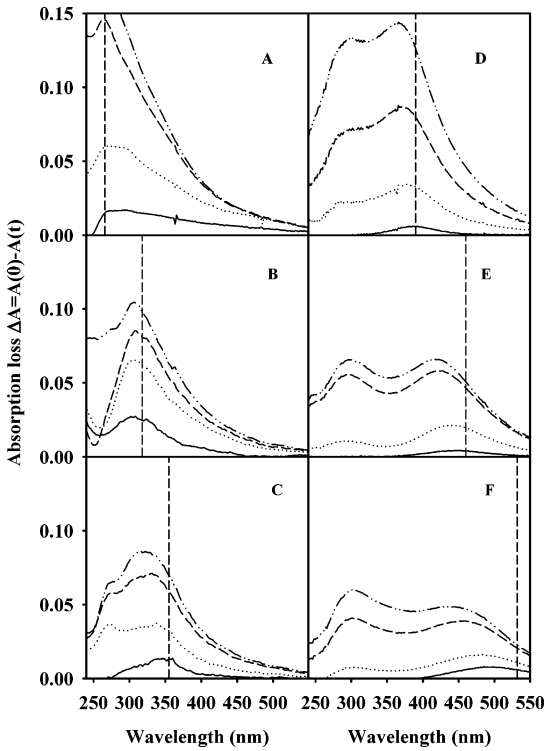

FIGURE 3. Time dependence of the absorption loss (ΔA) for SRHA upon exposure to laser irradiation (10 Hz): (A) at 266 nm (35 mJ/pulse) (10−580 s); (B) at 318 nm (6 mJ/pulse) (5−252 min); (C) at 355 nm (68 mJ/pulse) (2−85 min); (D) at 390 nm (5 mJ/pulse) (3−215 min); (E) (460 nm) (10 mJ/pulse) (0.3−312 min); and (F) (532 nm) (220 mJ/pulse) (10−3420 s). Vertical dashed lines represent irradiation wavelengths. Irradiation times: t_1 (—), t_2 (·····), t_3 (− −), t_4 (−··−).

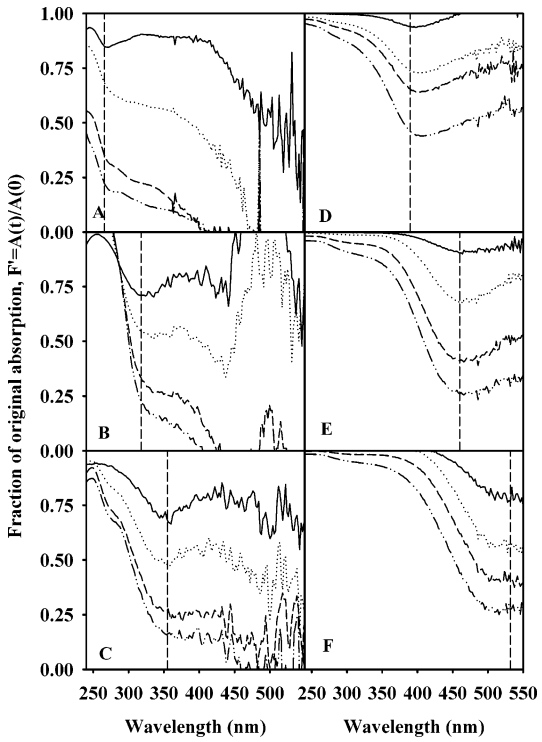

FIGURE 4. Time dependence of the fraction of original absorption (F′) for SRFA upon exposure to laser irradiation (10 Hz): (A) at 266 nm (35 mJ/pulse) (10−580 s); (B) at 318 nm (6 mJ/pulse) (5−252 min); (C) at 355 nm (68 mJ/pulse) (2−85 min); (D) at 390 nm (5 mJ/pulse) (3−215 min); (E) (460 nm) (10 mJ/pulse) (0.3−312 min); and (F) (532 nm) (220 mJ/pulse) (10−3420 s). Vertical dashed lines represent irradiation wavelengths. Irradiation times: t_1 (—), t_2 (·····), t_3 (− −), t_4 (−··−).

at these longer wavelengths without the appearance of distinct bands. Unlike the bands lost at λ_{irr}, which broadened and blue-shifted with increasing irradiation time, the 300 nm band always showed a constant wavelength maximum that was independent of λ_{irr} ($\lambda_{irr} \geq 390$ nm) and irradiation time. Moreover, substantial product absorption bands were observed upon direct irradiation into this band ($\lambda_{irr} = 318$ nm). These results argue that a distinct chromophore, or a closely related class of chromophores, underlies this band. Interestingly, at comparable absorption losses at 300 nm, a greater amount of product absorption was observed upon direct irradiation into this band (e.g., Figure 2B) as compared with irradiation at $\lambda \geq 390$ nm (e.g., Figure 2D−E). This result suggests that the loss of the 300 nm band proceeds through different photochemical routes depending on the irradiation wavelength.

These results, like those from the luminescence measurements, are inconsistent with a superposition model. First, it is highly unlikely that a set of independent compounds absorbing at differing wavelengths within the long wavelength absorption tail ($\lambda_{irr} \geq 390$ nm) would all have in common a higher energy absorption band centered at 300 nm. Second, at short irradiation times, absorption losses were only observed in a broad hole at or near λ_{irr} (for $\lambda_{irr} \geq 390$ nm); distinct higher (or lower) energy absorption bands were not evident as would be expected for most common organic chromophores (see Supporting Information). Only at longer irradiation times did the 300 nm band appear, indicating that it is coupled with the species giving rise to the long wavelength absorption tail but not linearly.

Fraction of Original Absorption (F′). We showed previously (*21*) that the following expression can be derived for a set of chromophores undergoing independent photobleaching

$$F' = A_T(t,\lambda)/A_T(0,\lambda) = \sum_i^n f_i(\lambda)\cdot e^{-\sigma_{P_i}(\lambda_{irr})\cdot E(\lambda_{irr})\cdot t} \qquad (1)$$

where $A_T(t,\lambda)$ and $A_T(0,\lambda)$ is the total absorption at observation wavelength λ for irradiation time t and time 0, respectively; $f_i(\lambda)$ is the fractional absorption contribution of the i^{th} chromophore at λ; $\sigma_{Pi}(\lambda_{irr})$ is the photobleaching cross section (cm^2 $photon^{-1}$) of the i^{th} chromophore, and E is the irradiance (photons cm^{-2} s^{-1}) at the irradiation wavelength (λ_{irr}). This equation assumes that the photobleaching of any one chromophore does not affect the bleaching of another, either through a sensitized photochemical process or through a change in electronic coupling (e.g., charge−transfer or energy−transfer). This equation further assumes that the photobleaching of a chromophore does not produce new chromophores that absorb over the spectral range of the observations, consistent with the results presented above for wavelengths >300 nm.

This equation provides several key predictions. First, for a single chromophore or for a system acting as a single chromophore, the decrease in F′ with time will be independent of wavelength. Second, for a system of chromophores undergoing independent photobleaching, reciprocity must hold between any two pairs of irradiation/observation wavelengths over the spectral range in which the chromophores absorb (*21*); namely, the fractional absorption losses observed at wavelength 1 when irradiated at wavelength 2 must be equivalent to those observed at wavelength 1 when irradiated at wavelength 1 and vice versa. Both of these predictions are supported by studies of model compounds (see Supporting Information).

Reciprocity is clearly violated for the HS (Figures 4 and 5). For example, following extensive photobleaching at

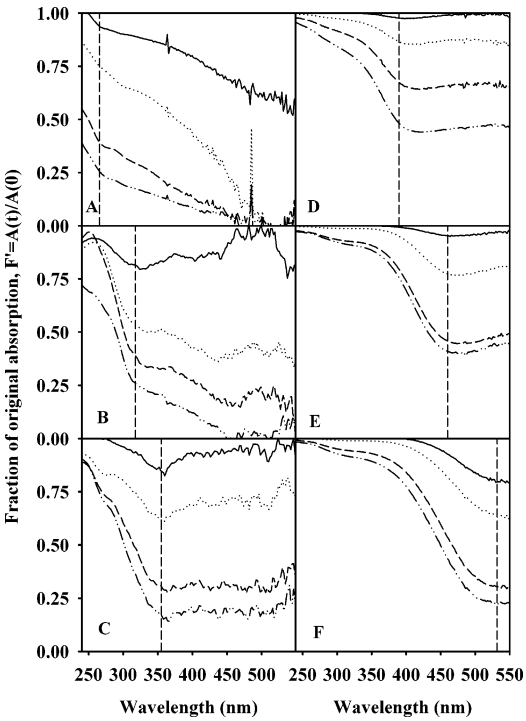

FIGURE 5. Time dependence of the fraction of original absorption (F′) for SRHA upon exposure to laser irradiation (10 Hz): (A) at 266 nm (35 mJ/pulse) (10−580 s); (B) at 318 nm (6 mJ/pulse) (5−252 min); (C) at 355 nm (68 mJ/pulse) (2−85 min); (D) at 390 nm (5 mJ/pulse) (3−215 min); (E) (460 nm) (10 mJ/pulse) (0.3−312 min); and (F) (532 nm) (220 mJ/pulse) (10−3420 s). Vertical dashed lines represent irradiation wavelengths. Irradiation times: t_1 (—), t_2 (·····), t_3 (– –), t_4 (—··—).

$\lambda_{irr} = 355$, the fractional absorption losses (1 − F′) at 355 and 532 nm were similar, ∼0.80−0.85 (t_4 in Figures 4C and 5C). In contrast, extensive irradiation at 532 nm produced a fractional absorption loss of ∼0.80 at 532 nm but only a ∼0.10 loss at 355 nm (t_4 in Figures 4F and 5F). Similar violations of reciprocity can be observed at other pairs of irradiation/observation wavelengths (Figures 4 and 5).

At very short irradiation times, the fractional absorption loss was centered in a band at λ_{irr} for all $\lambda_{irr} \geq 355$ nm (Figures 4 and 5). However, at longer irradiation times, the fractional absorption loss increased substantially at wavelengths to the red of λ_{irr}. At long irradiation times, F′ became nearly independent of wavelength for all $\lambda \geq \lambda_{irr}$, particularly for SRHA (Figures 4C−F and 5C−F). As discussed previously, this behavior is characteristic of systems photobleaching as a single unit or species and is the principal cause of the reciprocity violations. These results, like those from the luminescence measurements, suggest strongly that the long wavelength absorption tail ($\lambda > 350$ nm) arises from a coupled manifold of states.

Discussion

This study has provided unequivocal evidence that a simple superposition model of HS optical properties cannot apply (*20*, *22*, *23*). Evidence that directly contradicts or is inconsistent with this model includes (1) the monotonically increasing emission maxima and decreasing luminescence quantum yields with increasing excitation wavelength, (2) the uncharacteristically low luminescence quantum yields, (3) the appearance of only a single photobleaching band (hole) at λ_{irr} ($\geq$390 nm) after short periods of laser irradiation, (4) the appearance of a common 300 nm band at all $\lambda_{irr} \geq 390$ nm following longer periods of laser irradiation, (5) the violation of reciprocity, and (6) the uniform photobleaching (wavelength independent F′) at wavelengths above λ_{irr} ($\geq$355 nm) at longer laser irradiation times.

Instead, these results are more consistent with an interaction model, which we propose results from intramolecular donor−acceptor interactions within the HS (*17*, *24*, *25*, *28*, *32*). As mentioned previously, optical charge−transfer bands can arise via a ground-state association between an electron donor (D) and an electron acceptor (A) to form a D−A charge−transfer complex. These D−A complexes exhibit new broad absorption bands that are not shown by either the D or A molecules alone. These bands arise from the partial or complete promotion of an electron from the donor to the acceptor upon absorption of a photon.

HS are known to contain D and A moieties that do produce charge−transfer bands in solution (*29*, *33*). Examples of D moieties include polyhydroxylated aromatics such as those found in lignin, as well as phenols and indoles, which can form charge−transfer bands with appropriate A moieties, such as quinones or other oxidized aromatics that are also known or thought to be part of HS (*1*). Because the absorption and emission properties of HS are largely independent of concentration, these charge−transfer bands would have to arise from intramolecular donor−acceptor interactions within the HS, most likely between donors and acceptors colocalized randomly on polymer chains (of variable length).

A simple energy level diagram that both illustrates our proposal and is consistent with much of the experimental data is provided in Scheme 1. Here $(DA)_1$ through $(DA)_n$ represent a series of differing intramolecular charge−transfer contacts that produce a continuum of lower energy optical transitions. We propose that longer polymer chains would have a greater number and variety of possible D−A contacts, thus leading to a broader ensemble of optical transition energies that would extend further into the visible wavelengths. The observation that the magnitude of absorption

SCHEME 1. Energy Level Diagram Representing the Donor (D), Acceptor (A), and a Continuum of Differing Intramolecular Charge Transfer Contacts $(DA)_1$ to $(DA)_n$ between D and A[a]

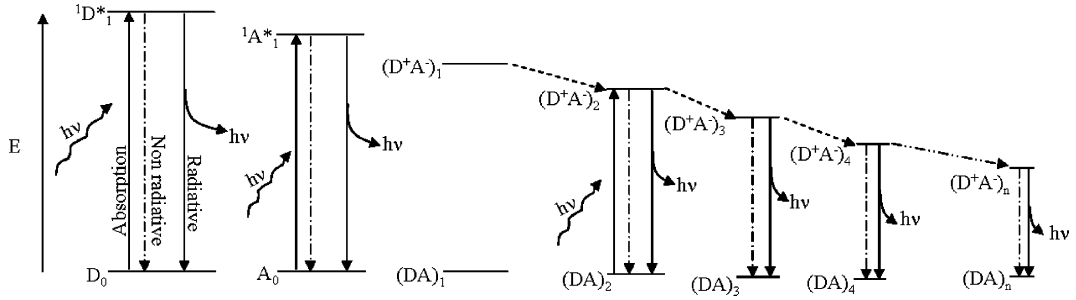

[a] D_0 and A_0 represent the ground states, $^1D^*_1$ and $^1A^*_1$ the first excited singlet states, and (D^+A^-) the charge transfer excited states. The dashed arrows represent the coupling between lower and higher energy charge transfer states. The scheme illustrates that excitation of specific charge transfer band ($(DA)_2 \rightarrow (D^+A^-)_2$) leads to emission (and photobleaching) from the lower-lying states populated via the excited state coupling. For simplicity, the coupling is shown as a sequential process, although these states could also be populated in parallel.

in the visible increases with increasing molecular weight of the HS is fully consistent with this idea (*7*, *17*, *39*). In addition to the charge−transfer transitions, higher energy transitions due to the D and A moieties alone (local states) will also contribute to the observed spectrum (Scheme 1). We attribute the 300 nm band to one of these classes of moieties, either D or A.

Consistent with the experimental results, this model predicts that laser irradiation into the 300 nm band will lead not only to the loss of the 300 nm band (either D or A) but also to the loss of all long-wavelength absorption due to the destruction of the D−A contacts. In contrast, irradiation into the charge-transfer bands (e.g., $\lambda_{irr} \geq 355$) leads initially to the selective destruction of only those D−A contacts whose transition energies correspond to the laser wavelength and thus produces a hole; because the number of D and A moieties contributing to these specific D−A contacts represents only a small fraction of the total population of D and A, little loss of the 300 nm band is observed at short laser irradiation times. Only at longer irradiation times, when the photobleaching extends across additional wavelengths, does this band appear due to greater D−A destruction.

Within this model (Scheme 1), the observation that the fractional absorption loss increases rapidly and becomes nearly wavelength independent at longer irradiation times for $\lambda \geq \lambda_{irr}$ ($\geq$355 nm) (Figures 4 and 5) requires that the lower energy transitions are coupled with those at higher energy (indicated by arrows in Scheme 1). This intramolecular coupling could arise through a number of mechanisms including energy transfer, charge migration, structural reorganization, or some combination of these. Indeed, the breadth of the holes at early irradiation times is likely due in part to one or more of these mechanisms. Some of these same mechanisms have been invoked to explain the absence of fluorescence line narrowing in laser-induced fluorescence measurements of HS at low temperature (*28*, *40*).

The luminescence measurements are also consistent with this model. First, the observation that emission spectra acquired at successively longer λ_{exc} always fall within the emission envelope of spectra acquired at shorter λ_{exc} (Figure 1C) argues that the emitting states populated by longer wavelength excitation are a lower energy subset of those populated by shorter wavelength excitation, and further, that these states are coupled (Scheme 1). Second, the monotonic decrease in emission quantum yields with increasing excitation wavelength can be explained by a simple energy gap argument; as the energy gap decreases, the rate of nonradiative relaxation increases relative the radiative rate (*41*).

What types of species could produce such behavior? Hernes and Benner (*42*) recently found that the absorption of chromophoric dissolved organic matter (i.e., HS) was highly correlated with its lignin phenol content. Because unaltered lignin is composed of hydroxy− (or methoxy−) benzene units, it will not absorb at long wavelengths (*43*). We propose, however, that oxidation of a portion of the hydroxy−benzene moieties to quinones or other similar oxidized species will incorporate acceptor groups randomly within the structure, thus leading to charge−transfer interactions between these donor (hydroxy−benzene) and acceptor (quinoid) groups. Precedence for this proposal has been obtained for oligomers and polymers of hydroquinones, where partial oxidation of the hydroquinone groups (D) to quinones (A) produces intramolecular charge−transfer bands (*44*−*46*). More recently, Klapper et al. (*47*) found that the long wavelength emission observed in a series of fulvic acids was almost completely eliminated following the microbial reduction of moieties, presumably quinones, within these materials. As many quinones undergo rapid intersystem crossing to the triplet and thus do not fluoresce (*48*, *49*), a reasonable explanation for the results of Klapper et al. (*47*) is that elimination of the acceptor groups (quinones) by reduction also eliminates the charge−transfer bands.

We believe that these donor−acceptor interactions may be a common phenomenon, occurring within all natural hydroxy− or polyhydroxy−aromatic polymers that form appropriate acceptors upon partial oxidation through either (bio)chemical (*1*) or photochemical (*50*) pathways. Examples of such species include lignin, polyphenols, tannins, and melanins. Future work will be directed to testing this proposal explicitly.

Acknowledgments

We thank Sean McElroy and Prof. Daniel Falvey for the use of and assistance with the laser. This work was supported by the Office of Naval Research.

Supporting Information Available

Results for an additional set of laser photobleaching experiments, which were performed on a series of model compounds, both alone and in a mixture, to test whether (i) sensitized photobleaching was observable in 90% glycerol/10% water, (ii) F′ was independent of wavelength for the photobleaching of single chromophores, and (iii) the photobleaching losses observed for a mixture of model compounds could be described as a simple sum of the absorption losses of the individual compounds. This material is available free of charge via the Internet at http://pubs.acs.org.

Literature Cited

(1) Stevenson, F. J. *Humus Chemistry. Genesis, Composition, Reactions*, 2nd ed.; John Wiley & Sons: New York, 1994.
(2) Schnitzer, M.; Khan, S. U. *Humic Substances in the Environment*; Marcel Dekker: New York, 1972.
(3) Hayes, M. H. B.; MacCarthy, P.; Malcolm, R. L.; Swift, R. S. *Humic Substances II: In Search of Structure*; John Wiley and Sons: New York, 1989.
(4) Aiken, G. R.; McKnight, D. M.; Wershaw, R. L.; MacCarthy, P. *Humic Subtances in Soil, Sediment, and Water*; John Wiley and Sons: New York, 1985.
(5) Zepp, R. G.; Schlotzhauer, P. F. *Chemosphere* **1981**, *10*, 479−486.
(6) Bricaud, A.; Morel, A.; Prieur, L. *Limnol. Oceanog.* **1981**, *26*, 43−53.
(7) Blough, N. V.; Del Vecchio, R. In *Biogeochemistry of Marine Dissolved Organic Matter*; Hansel, D. A., Carlson, C. A., Eds.; Academic Press: San Diego, 2002; pp 509−546.
(8) Green, S. A.; Blough, N. V. *Limnol. Oceanog.* **1994**, *39*, 1903−1916.
(9) Blough, N. V.; Zafiriou, O. C.; Bonilla, J. *J. Geophys. Res.* **1993**, *98*, 2271−2278.
(10) de Mora, S.; Demers, S.; Vernet, M. *The Effects of UV Radiation in the Marine Environment*; Cambridge University Press: Cambridge, 2000.
(11) Hader, D. P.; Kumar, H. D.; Smith, R. C.; Worrest, R. C. *Photochem. Photobiol. Sci.* **2003**, *2*, 39−50.
(12) Bidigare, R. R.; Ondrusek, M. E.; Brooks, J. M. *J. Geophys. Res* **1993**, *98*, 2259−2269.
(13) Arrigo, K. R.; Brown, C. W. *Mar. Ecol.: Prog. Ser.* **1996**, *140*, 207−216.
(14) Mopper, K.; Kieber, D. J. In *Biogeochemistry of Marine Dissolved Organic Matter*; Hansel, D. A., Carlson, C. A., Eds.; Academic Press: San Diego, 2002; pp 455−507.
(15) Blough, N. V.; Zepp, R. G. In *Active Oxygen in Chemistry*; Foote, C. S., Valentine, J. S., Greenberg, A., Liebman, J. F., Eds.; Champman and Hall: New York, 1995; pp 280−333.
(16) Blough, N. V. In *The Sea Surface and Global Change*; Liss, P. S., Duce, R. A., Eds.; Cambridge University Press: Cambridge, 1997; pp 383−424.
(17) Blough, N. V.; Green, S. A. In *The Role of Nonliving Organic Matter in the Earth's Carbon Cycle*; Zepp, R. G., Sonntag, C., Eds.; John Wiley and Sons: Chichester, 1995; pp 23−45.
(18) Kalle, K. *Ocean Mar. Biol. Annu. Rev.* **1966**, *4*, 91−104.
(19) Hojerslev, N. In *The Role of Solar Ultraviolet Radiation in Marine Ecosystems*; Calkins, J., Ed.; Plenum Press: New York, 1982; pp 263−281.

(20) Goldstone, J. V.; Del Vecchio, R.; Blough, N. V.; Voelker, B. M. *Photochem. Photobiol.* ASAP, DOI: 10.1562/TM-03-17.
(21) Del Vecchio, R.; Blough, N. V. *Mar. Chem.* **2002**, *78*, 231−253.
(22) Boehme, J. R.; Coble, P. G. *Environ. Sci. Technol.* **2000**, *34*, 3283−3290.
(23) Stedmon, C. A.; Markager, S.; Bro, R. *Mar. Chem.* **2003**, *82*, 239−254.
(24) Korshin, G. V.; Li, C. W.; Benjamin, M. M. *Water Res.* **1997**, *31*, 1787−1795.
(25) Power, J. F.; Langford, C. H. *Anal. Chem.* **1988**, *60*, 842−846.
(26) Korshin, G. V.; Kumke, M. U.; Li, C. W.; Frimmel, F. H. *Environ. Sci. Technol.* **1999**, *33*, 1207−1212.
(27) Jones, G.; Indig, G. L. *New J. Chem.* **1996**, *20*, 221−232.
(28) Ariese, F.; van Assema, S.; Gooijer, C.; Bruccoleri, A. G.; Langford, C. H. *Aquat. Sci.* **2004**, *66*, 86−94.
(29) Slifkin, M. A. *Charge−transfer interaction of biomolecules*; Academic Press: London, 1971.
(30) Birks, J. B. In *Photophysics of aromatic molecules*; Wiley-Interscience: New York, 1970; pp 403−414.
(31) Turro, N. J. *Modern Molecular Photochemistry*; University Science Books: Herndon, VA, 1991.
(32) Korshin, G. V.; Benjamin, M. M.; Li, C. W. *Water Sci. Technol.* **1999**, *40*, 9−16.
(33) Michaelis, L.; Granick, S. *J. Am. Chem. Soc.* **1944**, *66*, 1023−1030.
(34) Zepp, R. G.; Schlotzhauer, P. F.; Sink, R. M. *Environ. Sci. Technol.* **1985**, *19*, 74−81.
(35) Cooper, W. J.; Zika, R. G.; Petasne, R. G.; Fischer, A. M. *ACS Symp. Ser.* **1989**, *219*, 333−362.
(36) Brinkmann, T.; Sartorius, D.; Frimmel, F. H. *Aquat. Sci.* **2003**, *65*, 415−424.
(37) White, E. M.; Vaughan, P. P.; Zepp, R. G. *Aquat. Sci.* **2003**, *65*, 402−414.
(38) Herbelin, S. E.; Blough, N. V. *J. Phys. Chem. B* **1998**, *102*, 8170−8176.
(39) Chin, Y. P.; Aiken, G.; O'Loughlin, E. *Environ. Sci. Technol.* **1994**, *28*, 1853−1858.
(40) Kumke, M. U.; Frimmel, F. H.; Ariese, F.; Gooijer, C. *Environ. Sci. Technol.* **2000**, *34*, 3818−3823.
(41) Jones, G. In *Photoinduced Electron Transfer, Part A*; Fox., M. A., Chanon, M., Eds.; Elsevier: Amsterdam, 1988.
(42) Hernes, P. J.; Benner, R. *J. Geophys. Res.* **2003**, *108*(C9), 3291.
(43) Schubert, W. L. *Lignin Biochemistry*; Academic Press: New York, 1965.
(44) Kamogawa, H.; Giza, Y. C.; Cassidy, H. G. *J. Polym. Sci., Part A: Polym. Chem.* **1964**, *2*, 4647.
(45) Moser, R. E.; Cassidy, H. G. *J. Org. Chem.* **1965**, *30*, 2602.
(46) Moser, R. E.; Cassidy, H. G. *J. Org. Chem.* **1965**, *30*, 3336.
(47) Klapper, L.; McKnight, D. M.; Fulton, J. R.; Blunt-Harris, E. L.; Nevin, K. P.; Lovley, D. R.; Hatcher, P. G. *Environ. Sci. Technol.* **2002**, *36*, 3170−3175.
(48) Pochon, A.; Vaughan, P. P.; Gan, D. Q.; Vath, P.; Blough, N. V.; Falvey, D. E. *J. Phys. Chem. A* **2002**, *106*, 2889−2894.
(49) Gorner, H. *Photochem. Photobiol.* **2003**, *78*, 440−448.
(50) Muller, U.; Ratzsch, M.; Schwanninger, M.; Steiner, M.; Zobl, H. *J. Photochem. Photobiol., B* **2003**, *69*, 97−105.

Received for review January 17, 2004. Revised manuscript received April 12, 2004. Accepted May 6, 2004.

ES049912H